Journal of The Electrochemical Society, **147** (6) 2385-2388 (2000)
S0013-4651(99)09-091-6 CCC: $7.00 © The Electrochemical Society, Inc.

Application of Electrostatic Bonding to Field Emission Display Vacuum Packaging

Duck-Jung Lee,[a,z] Nam-Yang Lee,[b] Sung-Jae Jung,[b] Kwan-Su Kim,[b] Yun-Hi Lee,[a] Jin Jang,[c,*] and Byeong-Kwon Ju[a]

[a]*Electronic Materials and Devices Research Center, Korea Institute of Science and Technology, Cheongryang, Seoul 130-650, Korea*
[b]*Orion Electric Company, Limited, Ajou University, Wonchun-dong, Suwon, Korea*
[c]*Department of Physics, Kyunghee University, Hoigi-dong, Dongdaemun-gu, Seoul 130-701, Korea*

A tubeless packaging technology for field emission display (FED) devices is developed using indirect glass-to-glass electrostatic bonding with an intermediate amorphous silicon layer at a low temperature of 230°C. The glass-to-glass bonding mechanism is investigated by secondary-ion mass spectroscopy. To evaluate the vacuum sealing capability of a FED panel packaged by this method, the leak characteristics of the vacuum were examined by spinning rotor gauge for 6 months and the electron emission properties of the panel was measured continuously for different amounts of time over a 26 day period. In order to examine the effect of the removal of the exhausting tube on the enhancement of vacuum efficiency, we have calculated a theoretical vacuum level in the panel based on conductance and throughput and compared with experimental values.
© 2000 The Electrochemical Society. S0013-4651(99)09-091-6. All rights reserved.

Manuscript submitted September 23, 1999; revised manuscript received February 18, 2000.

Field emission display (FED) is one of the most promising flat panel displays (FPDs). The advantages of FED devices are well known; wide viewing angle, fast response time, low power consumption, and wide operating temperature range.[1,2] However, a FED panel is normally operated in high vacuum environments to provide long-term performance and ensure reliability. In general, FED panels have been packaged by the cathode ray tube (CRT) like method that has been proved to be limited in terms of the out-gassing and metal oxidation by high-temperature processes, and the lower vacuum conductance due to small inner volume.[8-10] The glass-to-glass bonding is the most promising method for solving the above mentioned problems as well as for realizing an ideal hermetic package. The bonding technique of substrates has been developed continuously for micromachining processes.[3,4] In particular, electrostatic bonding provides a strong hermetic seal and protection to the devices from the surrounding effects in spite of a relatively simple process. It was invented in 1969 by Wallis and Pomerantz, and has mainly focused on the bonding of silicon–to-Pyrex no. 7740 glass.[5,6]

This paper reports the indirect glass-to-glass bonding technology based on conventional silicon-glass anodic bonding mechanism using amorphous silicon film for fabrication a high vacuum sealed 1.25 in. FED panel. With this method, we can achieve the shorter pumping time and higher vacuum level under low temperatures. If the vacuum packaging of FED, plasma display panel (PDP), and sensors can be replaced by glass-to-glass bonding, it will become possible to take advantage of the low cost, low package temperature, and high vacuum efficiency this process offers.

Experimental

In this work, a soda-lime glass substrates was chosen as a base plate because of low permeation rate, which is the transfer rates of gas from the high pressure side to the low pressure side.[7] Normally, Pyrex no. 7740 glasses are used for anodic bonding because the thermal expansion coefficient is well matched to that of a silicon wafer. However, such glasses cannot maintain the high vacuum level necessary for long periods of time due to its high permeation rate.[11] Therefore, soda-lime glass with low permeation rate is used for high vacuum devices such as CRT, vacuum fluorescent display (VFD), FED, etc.

An amorphous silicon film was deposited by radio-frequency (rf)-magnetron sputtering at 120°C on indium-tin oxide (ITO) coated soda-lime glass. Then, the bare soda-lime glass was contacted on amorphous silicon film, as shown in Fig. 1. The ITO film provides planar contact and homogeneous electric field distribution during bonding. At elevated temperatures, mobility of the positive sodium ions in the glass was fairly high and the presence of an electric field caused them to migrate to the negatively charged cathode at the back of the glass wafer. As the Na^+ ions migrated toward the cathode, they left behind fixed charges (mainly oxygen ions) in the glass, creating a high electrostatic field with image charge in the amorphous silicon. As a consequence, the contacted glasses pulled the surfaces together and were presumed to occur at atomic bonds as Si–O–Si.[8] The indirect glass-to-glass bonding mechanism was investigated by secondary-ion mass spectroscopy (SIMS).

Figure 2a shows the schematic structure of the tubeless FED panel by the proposed method. The capping glass was bonded to the amorphous silicon film deposited around the hole in the back side of the panel and, as a result, a hermetic seal of FED could be obtained. Figure 2b shows the magnified image of Mo-tip field emitter arrays (FEA), which was fabricated on n-type silicon (100) wafer by spindt method.[9]

The exhaust hole was 6 mm diam, the gate and cathode electrode lines of chromium were formed on cathode glass plate. Then, the FEAs fabricated on the silicon wafer were mounted on the cathode electrode lines of cathode glass followed by gate lines of FEAs connected to the electrode lines of the cathode glass plate by wire-bonding. The ZnO:Zn phosphor was printed and the glass frit was dispensed on the anode glass plate. The ZnO:Zn phosphor was then placed on the cathode glass plate and heated to 470°C to melt a glass

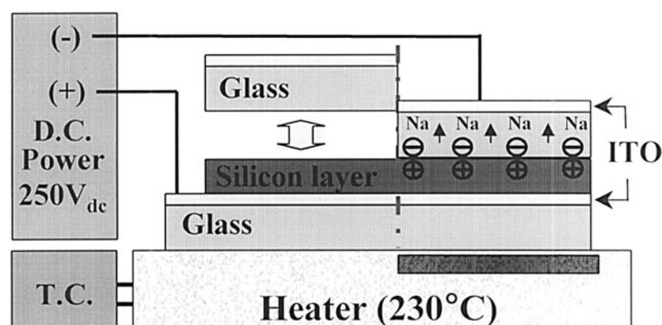

Figure 1. Experimental setup and mechanism for indirect glass-to-glass bonding.

* Electrochemical Society Active Member.
[z] E-mail: djlee@kist.re.kr

Downloaded 30 Jun 2008 to 163.152.52.85. Redistribution subject to ECS license or copyright; see http://www.ecsdl.org/terms_use.jsp

S0013-4651(99)09-091-6 CCC: $7.00 © The Electrochemical Society, Inc.

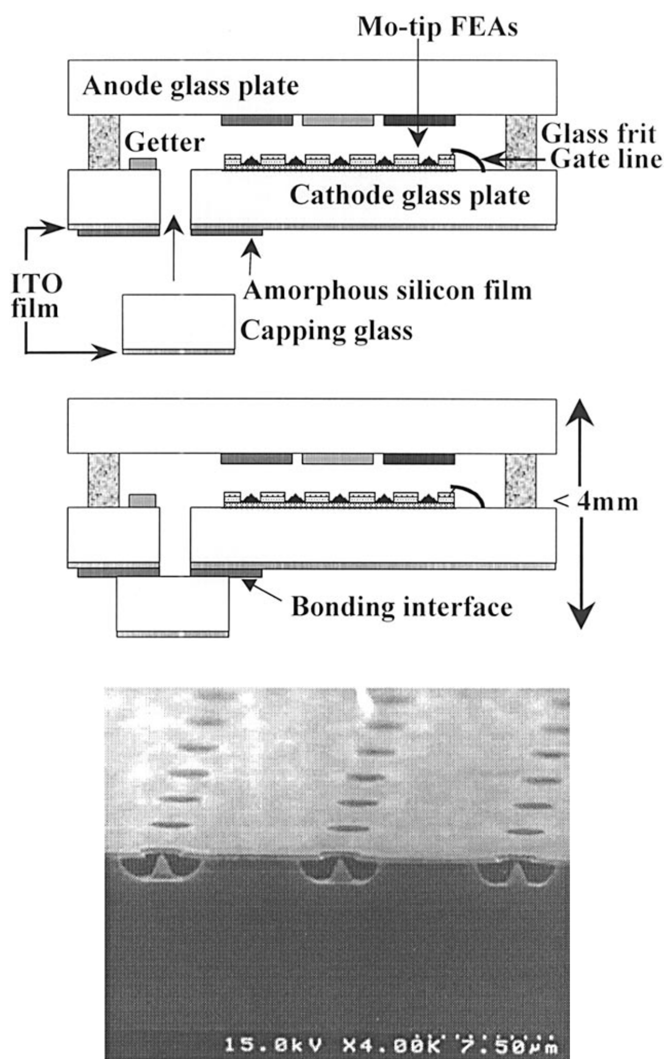

Figure 2. Geometrical structure of (a) tubeless packaged FED and (b) cross-sectional view.

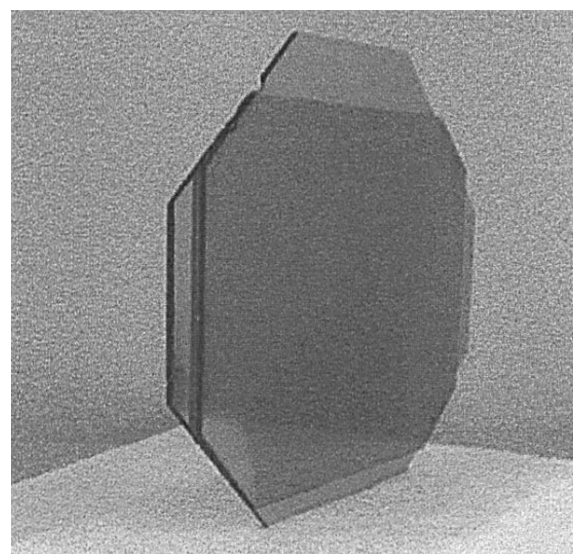

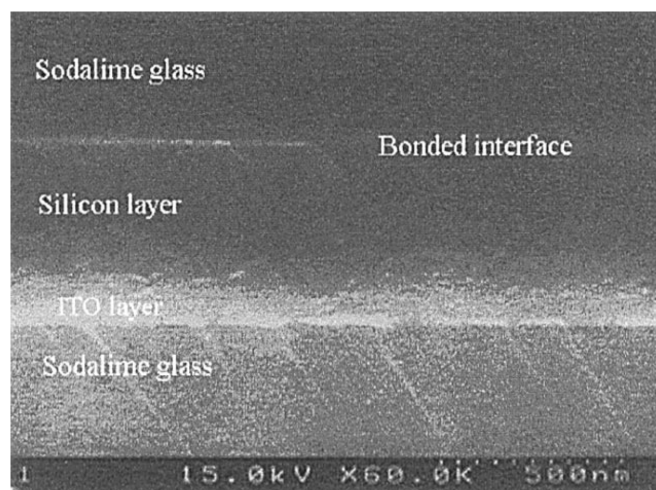

Figure 3. Image of bonded glass pairs; (a) optical view and (b) cross-sectional view.

frit in N_2 ambient. However, the panel with the open exhaust hole was successfully fabricated as mentioned above. Then an amorphous silicon film 200 nm thick was deposited around the hole of the back side panel. A sheet type getter (ST122) was inserted into the panel through the exhaust hole. Finally, the amorphous silicon film on the panel and a capping (bare) glass was bonded successfully at 230°C with bias of 250 V_{dc} in a vacuum chamber under 1×10^{-6} Torr. To observe the hermetic sealing capability of tubeless packaged FED panels, the inner vacuum level was measured using spinning rotor gauge (SRG).[10] The characteristics of light emission and stability for time variation were observed from tubeless packaged 1.25 in. FED panel.

Results and Discussion

Glass-to-glass electrostatic bonding.—Figure 3a shows the glass-to-glass bonded pairs. The bonded areas appear as a dark gray color in whole upper glass plates. The bonded samples were cut to investigate the bonded interface region. Figure 3b shows the cross-sectional scanning electron microscopy (SEM) images of the cut glass pairs. The bonded interface region between amorphous silicon film and bare glass was smooth and clearly defined. When bare glass was pulled from bonded pairs by tensile strength, fracturing was seen at the bulk region of the glass or the interface region between ITO film and an amorphous silicon film. To investigate the compositional change at the interface region after the bonding process, SIMS analysis was carried out at the fracturing at the interface. The depth profiles were obtained continuously with the sputtering rate of 10 nm/min for the amorphous silicon film and bonded glass substrates, as shown in Fig. 4. In the amorphous silicon film, the lower ion counts result from the difference ionization rate of film for sputtering of SIMS analysis.

The depletion region of sodium and potassium was observed in the glass surface upto a depth of ~500 nm. This region is the source of the electrostatic force that pulls both glass plates. The depletion region of soda-lime glass of alkali-rich was deeper than that of Pyrex glass. Also, the reaction region with increasing Si_2O and SiO bond was clearly observed in the glass side from a surface depth of 200 nm. We suppose that this could be explained by formation of Si–O originating from silicon oxidation by electrostatic force at interface.[11-14]

Emission characteristics of tubeless packaged FED.—The tubeless packaging of the panel was achieved successfully at 230°C with an applied bias of 250 V_{dc} in a vacuum chamber under 1×10^{-6} Torr. Figure 5a shows the light emission generated from tubeless packaged 1.25 in. FED panel when a gate bias of 90 V and anode bias of 350 V was applied to the panel. To examine the emission stability over a period of time, an external bias signal was applied to one line constantly as the ON for 45 min and OFF for 15 min for 26 days, as shown in Fig. 5b. Through fluctuation of the initial emission current during the first 8 days, a stable emission was maintained for the operating time variation afterward except for the some

Downloaded 30 Jun 2008 to 163.152.52.85. Redistribution subject to ECS license or copyright; see http://www.ecsdl.org/terms_use.jsp

S0013-4651(99)09-091-6 CCC: $7.00 © The Electrochemical Society, Inc.

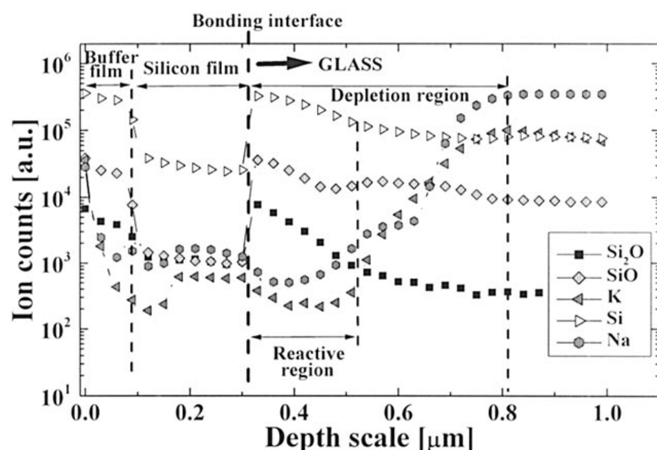

Figure 4. SIMS depth profiles of the amorphous silicon film on glass substrate after bonding process.

emissive vibration. To test the leakage probability for the tubeless packaged panel, we fabricated a test panel with two exhaust holes. One of the holes was connected directly to the SRG by a glass frit and the other was bonded in a vacuum environment by applying the

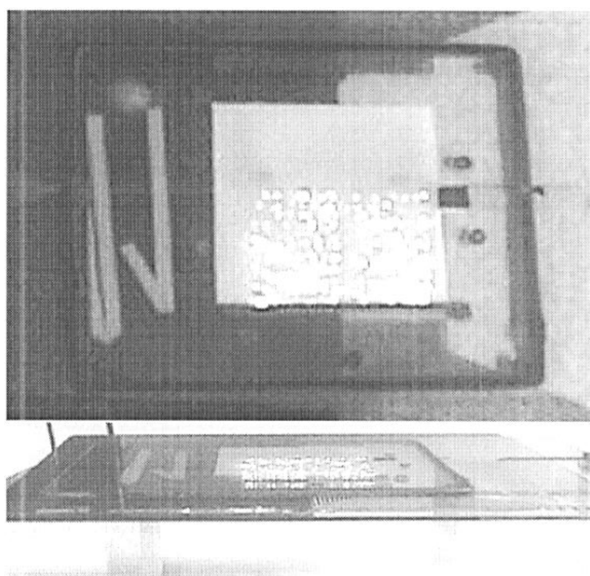

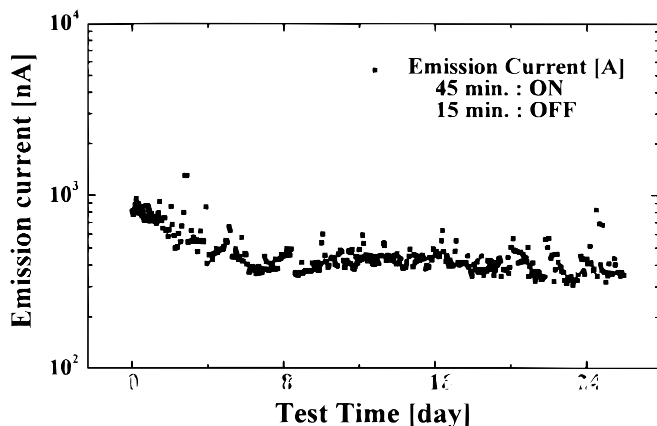

Figure 5. Emission characteristics for tubeless packaged 1.25 in. FED; (a, top) front and side view of light emission and (b, bottom) emission stability for time variation.

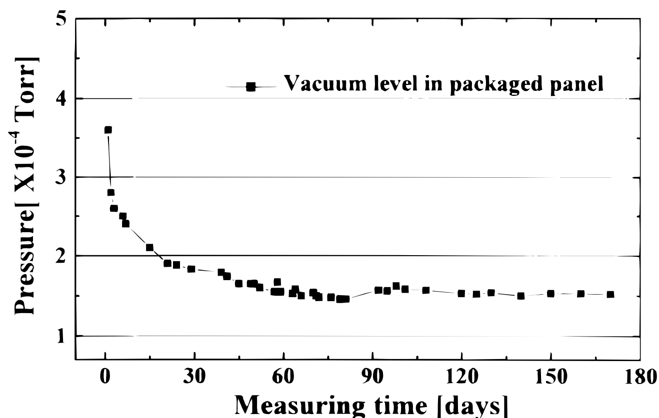

Figure 6. Inner pressure graph for packaged panel by spinning rotor gauge.

process described above without getter. The value of inner pressure measured by SRG was input into the computer via an RS 232 port. Figure 6 shows that the pressure maintained a vacuum level under 10^{-4} Torr for 6 months. Because there is no leakage through the bonding interface, it should be possible to apply this technology to vacuum packaged devices.

Vacuum efficiency of tubeless packaging.—Our method did not require an exhaust tube, which is used in conventional CRT vacuum packaging. The method has some advantages, such as decrease of panel thickness and increase of vacuum efficiency. To examine the enhancement of vacuum efficiencies of the removal of the exhaust tube, we calculated a theoretical vacuum level in the panel based on concepts such as conductance and throughput using Eq. 1-3. Here, throughput [Q] is defined as the product of pumping speed [S] and the inlet pressure [P], *i.e.*

$$Q = P_1 \times S_1 = P_2 \times S_2 = ... = P_n \times S_n \quad [1]$$

Q is the same all over the system. In Eq. 1, S is related with the conductance [C], which is the ability of the pipe to allow a unit volume of gas to pass through in a specified amount of time. For circular tubes, conductance becomes[15,16]

$$C_{\text{length}} = 12.1 \times D^3/L,\ C_{\text{orifice}} = 11.7 \times A \quad [2]$$

where D is diagonal, L is length, and A is area

$$1/C_{\text{tube}} = 1/C_{\text{length}} + 1/C_{\text{orifice}} \quad [3]$$

As described, the total conductance of the system was calculated from Eq. 3. When we used a 2 mm diam and 4 cm long tube, conductance of the tube was $\sim$0.019 ℓ/s and that of a 6 mm diam hole was estimated at 2.9 ℓ/s. Based on the calculated result, we expected an increase in conductance of about 153 times. Figure 7a shows the model system used to simulate an inner pressure of the panel. Figure 7b shows both the results, which were the values calculated by Eq. 3 and the values measured by a ion gauges 1 and 2. Ion gauge 1 was connected directly to the vacuum chamber and ion gauge 2 was connected through the exhaust tube, as shown in Fig.7a. From the results, we can see that the calculated value (2 mm tube) is well matched to the value measured by ion gauge 2. Therefore, we can estimate that vacuum level of a tubeless panel (tubeless) is about 10^{-6} Torr, when gauge 1 is 5×10^{-7} Torr. From this result, we conclude that the tubeless packaging method can achieve a higher vacuum level than can the exhaust tube under the same conditions.

Conclusion

Glass-to-glass electrostatic bonding with an intermediate amorphous silicon film has been developed for high vacuum packaging of the FED panel. We observed a depletion region of alkali ions in bulk glass and a reaction region of Si–O bond in interface from SIMS depth profile. The light emission was stable for the time period measured over 26 days from the packaged 1.25 in. FED panel. The

Downloaded 30 Jun 2008 to 163.152.52.85. Redistribution subject to ECS license or copyright; see http://www.ecsdl.org/terms_use.jsp

S0013-4651(99)09-091-6 CCC: $7.00 © The Electrochemical Society, Inc.

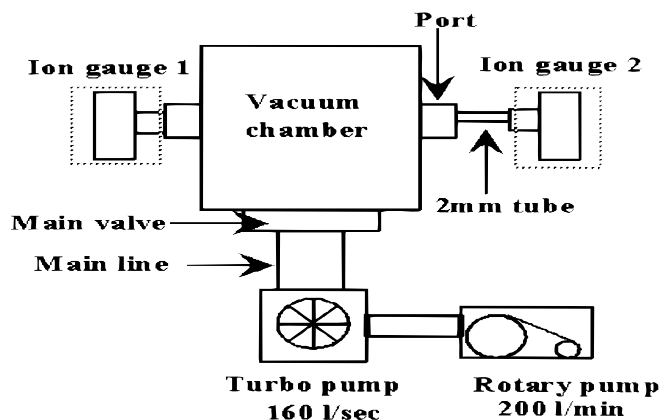

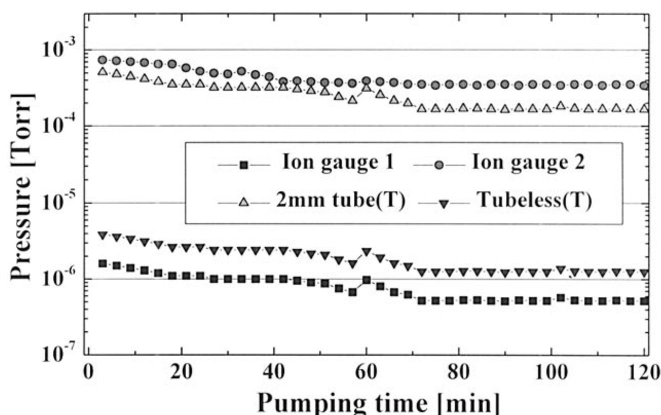

Figure 7. (a, top) Schematic diagram for vacuum level test in panel by system modeling. (b, bottom) Comparison of measured pressure (ion gauge 1, 2) and calculated pressure. T is a theoretical value.

vacuum level of the panel was kept constant for more than three months. From system modeling, we obtained a higher vacuum efficiency, more than 153 times increased conductance and ~200 times modified vacuum level, over those of the conventional packaging method. This new bonding method can be successfully applied to the hermetic seal of vacuum microelectronic devices. Also, it can be used for the low temperature processing, hermetic, and thin thickness packaging.

Acknowledgments

This research was supported by the Ministry of Science and Technology and the Ministry of Industry and Energy under Micromachinine Technology Development Program.

The Korea Institute of Science and Technology assisted in meeting the publication costs of this article.

Reference

1. P. H. Holloway, J. Sebastain, T. Trottier, H. Swartand, and R. O. Petersen, *Solid State Technol.*, 47 (1995).
2. L. Branst and F. Pothoven, *Solid State Technol.*, 109 (1996).
3. B. Puers, E. Peeters, A. Van Den Bossche, and W. Sensen, *Sens. Actuators A*, **21-23**, 8 (1990).
4. B. Puers and D. Lapadatu, *Sens. Actuators A*, **41-42**, 129 (1994).
5. C. D. Fung, P. W. Cheung, W. H. Ko, and D. G. Fleming, *Micromachining and Micropackaging of Transducers*, p. 41, Elsevier Science, Amsterdam (1985).
6. G. Wallis and D. I. Pomerantz, *J. Appl. Phys.,* **40**, 3946 (1969).
7. J. F. O'Hanlon, *A User's Guide to Vacuum Technology*, p. 292, 446, John Wiley & Sons, New York (1989).
8. Y. Kanda, K. Matsuda, C. Muraya, and J. Sugaya, *Sens. Actuators, A*, **21-23**, 939 (1990).
9. C. A. Spindt, I. Brodie, L. Humphrey, and E. R. Westerberg, *J. Appl. Phys.,* **47**, 5248 (1976).
10. S. J. Jung, G. J. Moon, K. S. Kim, M. S. Kim, K. J, Woo, N. Y. Lee, and S. Ahn, *ASID'98* proceedings, 1157 (1998).
11. P. Nitzsche, K. Lange, B. Schmidt, S. Grigull, and U. Kreissig, *J. Electrochem. Soc.*, **145**, 1755 (1998).
12. H. Baumann, S. Mack, and H. Munzel, in *Semiconductor Water Bonding: Physics and Applications III*, C. E. Hunt, H. Baumgart, S. S. Iyes, T. Abe, and U. Gösele, Editors, PV 95-7, p. 471, The Electrochemical Society Proceedings Series, Pennington, NJ (1995).
13. A. Cozma and B. Puers, *J. Micromech. Microeng*., **5**, 98 (1995).
14. Robert H. Doremus, *Glass Science*, p. 216, John Wiley & Sons Inc., New York, (1994).
15. A. Roth, *Vacuum Technology*, p. 62, Elsevier Science, Amsterdam (1990).
16. M. Ohring, *The Materials Science of Thin Films*, p. 57, Academic Press, Boston (1992).

Downloaded 30 Jun 2008 to 163.152.52.85. Redistribution subject to ECS license or copyright; see http://www.ecsdl.org/terms_use.jsp